PERGAMON

Chemical Engineering Science 57 (2002) 2885–2899

Chemical Engineering Science

www.elsevier.com/locate/ces

Diffusiophoresis of a colloidal sphere in nonelectrolyte gradients parallel to one or two plane walls

Po Y. Chen, Huan J. Keh *

Department of Chemical Engineering, National Taiwan University, Taipei 106-17, Taiwan, ROC

Received 8 January 2002; received in revised form 8 April 2002; accepted 25 April 2002

Abstract

The quasisteady diffusiophoretic motion of a spherical particle in a fluid solution of a nonionic solute located between two infinite parallel plane walls is studied theoretically in the absence of fluid inertia and solute convection. The imposed solute concentration gradient is constant and parallel to the two plane walls, which may be either impermeable to the solute molecules or prescribed with the far-field concentration distribution. The particle–solute interaction layer at the particle surface is assumed to be thin relative to the particle radius and to the particle–wall gap widths, but the polarization effect of the diffuse solute in the thin interfacial layer caused by the strong adsorption of the solute is incorporated. The presence of the neighboring walls causes two basic effects on the particle velocity: first, the local solute concentration gradient on the particle surface is enhanced or reduced by the walls, thereby speeding up or slowing down the particle; secondly, the walls increase viscous retardation of the moving particle. To solve the continuity and momentum equations, the general solutions are constructed from the fundamental solutions in both the rectangular and the spherical coordinate systems. The boundary conditions are enforced first at the plane walls by the Fourier transforms and then on the particle surface by a collocation technique. Numerical results for the diffusiophoretic velocity of the particle relative to that under identical conditions in an unbounded fluid solution are presented for various values of the relaxation parameter of the particle as well as the relative separation distances between the particle and the two plates. For the special case of diffusiophoretic motions of a spherical particle parallel to a single plate and on the central plane of a slit, the collocation results agree well with the approximate analytical solutions obtained by using a method of reflections. The presence of the lateral walls can reduce or enhance the particle velocity, depending on the surface properties of the particle, the relative particle–wall separation distances, and the solutal boundary condition at the walls. In general, the boundary effect on diffusiophoresis is quite complicated and relatively weak in comparison with that on sedimentation.

Keywords: Diffusiophoresis; Colloidal phenomena; Fluid mechanics; Diffusion; Boundary effects; Electrophoresis

1. Introduction

A colloidal particle can be driven to move by the application of a nonuniform solute concentration field that interacts with the surface of the particle. This phenomenon, known as diffusiophoresis (Dukhin & Derjaguin, 1974), has been demonstrated experimentally for both charged (Ebel, Anderson, & Prieve, 1988) and uncharged (Staffeld & Quinn, 1989) solutes. In a solution of nonionic solute with constant concentration gradient ∇C_∞, the diffusiophoretic velocity of a particle is (Anderson, Lowell, & Prieve, 1982)

$$\mathbf{U}^{(0)} = \frac{kT}{\eta} L^* K \nabla C_\infty \tag{1}$$

and there is no rotational motion of the particle. In the above equation, L^* is a characteristic length for the particle–solute interaction (of order 1–10 nm), K is the Gibbs adsorption length characterizing the strength of the adsorption of the molecular solute [K and L^* are defined later by Eqs. (6b) and (6c)], η is the fluid viscosity, k is Boltzmann's constant, and T is the absolute temperature. Eq. (1) can be applied to an isolated rigid particle of arbitrary shape and size. However, its validity is based on the assumption that the local radii of curvature of the particle are much larger than the thickness of the particle–solute interaction layer (diffuse layer) at the particle surface (of the same order as L^*) and the effect of the "polarization" of the diffuse solute (the solute continually adsorbs at the upstream edge and desorbs at the downstream edge) in the interfacial layer surrounding the particle is negligible.

* Corresponding author. Fax: +886-2-2362-3040.
E-mail address: huan@ccms.ntu.edu.tw (H. J. Keh).

0009-2509/02/$ - see front matter
PII: S0009-2509(02)00180-X

In the past decade, important advances have been made in the evaluation of the effect of diffuse-layer polarization on the diffusiophoretic velocity of colloidal particles. Anderson and Prieve (1991) analyzed the diffusiophoresis of a colloidal sphere of radius a with a thin but polarized diffuse layer at the particle surface when the suspending nonelectrolyte solution is only slightly nonuniform in solute concentration on the length scale of a ($a|\nabla C_\infty| \ll C_\infty$). They obtained for the diffusiophoretic velocity of the spherical particle as

$$\mathbf{U}_0 = A\nabla C_\infty, \tag{2a}$$

where the particle's mobility

$$A = \frac{kT}{\eta} L^* K \left(1 + \frac{\beta}{a}\right)^{-1} \tag{2b}$$

and the definition of the length β is given by Eq. (5). For a strongly adsorbing solute (e.g., a surfactant), the relaxation parameter β/a (or K/a) can be much greater than unity. If all the adsorbed solute were "stuck" to the surface of the particle (the diffuseness of the adsorption layer disappears), then $L^* = 0$ and there would be no diffusiophoretic migration of the particle. In the limit of $\beta/a \to 0$ (very weak adsorption), the polarization of the diffuse solute in the interfacial layer vanishes and Eq. (2) reduces to Eq. (1). It can be seen from Eqs. (1) and (2) that the effect of polarization of the diffuse layer is to lower the diffusiophoretic mobility of the particle. The reason for this consequence is that the transport of the solute inside the particle–solute interaction layer reduces the concentration gradient along the particle surface. It has been shown that Eq. (2) with no particle rotation holds even if ∇C_∞ varies appreciably over length scales comparable to the particle radius, with ∇C_∞ evaluated at the position of the particle center (Keh & Luo, 1995).

In practical applications of diffusiophoresis, colloidal particles usually are not isolated and will move in the presence of neighboring particles and/or boundaries. In the limiting case that Eq. (1) is applicable, the normalized velocity field of the unbounded fluid that is dragged by a particle during diffusiophoresis is the same as for electrophoresis of the dielectric particle with an infinitesimally thin electric double layer (Anderson, 1989); thus, the boundary effects on electrophoresis, which have been investigated extensively in the past and summarized by a review article (Chen & Keh, 1999), can be utilized to interpret those on diffusiophoresis.

When the polarization effect of solute species in the diffuse layer surrounding the particle is considered, the boundary effects on diffusiophoresis can be quite different from those on electrophoresis, due to the fact that the particle size and some other unique factors are involved in each transport mechanism. Through the use of a boundary collocation technique, the diffusiophoretic (and electrophoretic) motion of a colloidal sphere with a thin but polarized diffuse layer in the direction perpendicular to a plane wall was examined (Keh & Jan, 1996). Recently, the two-dimensional diffusiophoresis of a cylindrical particle with a thin polarized diffuse layer in a transversely imposed gradient of a nonionic solute near a plane wall has been analyzed using cylindrical bipolar coordinates in two fundamental cases: motion normal to the plane and motion parallel to the plane (Keh & Hsu, 2000).

The objective of this article is to obtain exact numerical solutions and approximate analytical solutions for the diffusiophoretic motions of a spherical particle with a thin but polarized diffuse layer in a solution of uncharged solute parallel to a single plane wall and to two plane walls at an arbitrary position between them. The plane walls may be either impermeable to the solute molecules or prescribed with the linear far-field solute concentration distribution, but the solute–wall interaction energy is assumed to be negligible. The effects of fluid inertia as well as solute convection are ignored. For the case of a particle with a small value of β/a undergoing diffusiophoresis near impermeable plane walls or of a particle with a large value of β/a undergoing diffusiophoresis near plane walls prescribed with the far-field concentration distribution, the solute diffusion around the particle will generate larger concentration gradients on the particle surface relative to those in an infinite medium. These gradients enhance the diffusiophoretic velocity, although their action will be retarded by the viscous interaction of the migrating particle with the walls. Both effects of this solutal enhancement and the hydrodynamic retardation increase as the ratios of the radius of the particle to its distances from the walls increase. Determining which effect is overriding at small particle–wall gap widths is a main target of this study.

2. Analysis

We consider the quasisteady diffusiophoresis of a spherical particle of radius a in a fluid solution of a nonionic solute parallel to two infinite plane walls whose distances from the center of the particle are b and c, as shown in Fig. 1. Here (x, y, z), (ρ, ϕ, z), and (r, θ, ϕ) denote the rectangular, circular cylindrical, and spherical coordinate systems, respectively, and the origin of coordinates is chosen at the particle center. A linear solute concentration field $C_\infty(x)$ with a uniform gradient $E_\infty \mathbf{e}_x$ ($=\nabla C_\infty$, where E_∞ is taken to be positive) is imposed in the surrounding fluid far away from the particle, where $\mathbf{e}_x$ together with $\mathbf{e}_y$ and $\mathbf{e}_z$ are the unit vectors in rectangular coordinates. It is assumed that the layer of interaction between the solute molecules and the particle surface is thin in comparison with the radius of the particle and the spacing between the particle and each wall. Hence, the fluid phase can be divided into two regions: an "inner" region defined as the thin interaction layer adjacent to the particle surface and an "outer" region defined as the remainder of the fluid phase. The objective is to determine the correction to Eq. (2) for the particle velocity due to the presence of the plane walls.

Before determining the diffusiophoretic velocity of the particle, the concentration and velocity fields in the fluid phase need to be found.

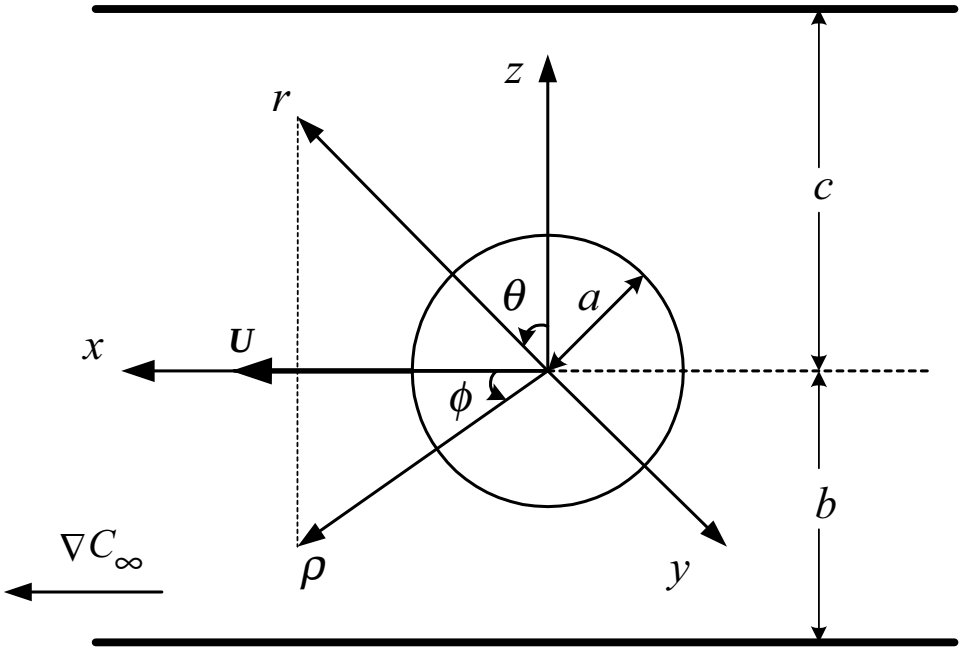

Fig. 1. Geometrical sketch for the diffusiophoresis of a spherical particle parallel to two plane walls at an arbitrary position between them.

2.1. Solute concentration distribution

The Peclet number of the system is assumed to be small. Hence, the equation of continuity governing the solute concentration distribution C for the outer region of the fluid solution of constant solute diffusivity is the Laplace equation,

$$\nabla^2 C = 0. \tag{3}$$

The above governing equation satisfies the boundary condition at the particle "surface" (outer limit of the thin interfacial layer) obtained by solving for the solute concentration in the inner region and using a matching procedure to ensure a continuous solution in the whole fluid phase (O'Brien, 1983; Anderson & Prieve, 1991),

$$r = a: \quad \frac{\partial C}{\partial r} = -\beta \left[\nabla^2 - \frac{1}{r^2}\frac{\partial}{\partial r}\left(r^2 \frac{\partial}{\partial r}\right)\right] C. \tag{4}$$

In the above equation, β is the relaxation coefficient defined by

$$\beta = (1 + vPe)K, \tag{5}$$

where

$$Pe = \frac{kT}{\eta D} L^* K C_0, \tag{6a}$$

$$K = \int_0^\infty [\exp(-\Phi(y_n)/kT) - 1]\, \mathrm{d}y_n, \tag{6b}$$

$$L^* = K^{-1} \int_0^\infty y_n [\exp(-\Phi(y_n)/kT) - 1]\, \mathrm{d}y_n \tag{6c}$$

and

$$v = (L^* K^2)^{-1} \int_0^\infty \left\{ \int_{y_n}^\infty [\exp(-\Phi(y_n)/kT) - 1] \times \mathrm{d}y_n \right\}^2 \mathrm{d}y_n. \tag{6d}$$

In Eq. (6), Φ represents the potential energy resulting from the interaction between a single solute molecule and the particle surface; D is the solute diffusion coefficient; y_n is the normal distance measured from the particle surface into the fluid phase; C_0 is the bulk concentration of the solute species measured at the particle center in the absence of the particle. To obtain Eqs. (4)–(6), it was assumed that the concentration of solute within the adsorption boundary layer is related to the solute–surface interaction energy by a Boltzmann distribution.

The solute concentration far away from the particle approaches the undisturbed values. Thus,

$$z = c, -b: \quad \frac{\partial C}{\partial z} = 0, \tag{7}$$

$$\rho \to \infty: \quad C = C_\infty = C_0 + E_\infty x. \tag{8}$$

Note that the boundary conditions given by Eq. (7) apply for the case of two impermeable plane walls (which can appear in practice) with negligible relaxation effect in their thin interfacial layers. For the case of diffusiophoretic motion of a particle parallel to two plane walls prescribed with a linear solute concentration profile consistent with the far-field distribution (which is less practical), Eq. (7) should be replaced by

$$z = c, -b: \quad C = C_0 + E_\infty x. \tag{9}$$

Since the governing equation and boundary conditions are linear, one can express the solute concentration distribution C, which is symmetric with respect to y and antisymmetric with respect to x, as the superposition

$$C = C_w + C_p. \tag{10}$$

Here, C_w is a double Fourier integral solution of Eq. (3) in rectangular coordinates that represents the disturbance produced by the plane walls plus the undisturbed concentration field and is given by

$$C_w = C_0 + E_\infty x + E_\infty \int_0^\infty \int_0^\infty (X\mathrm{e}^{\kappa z} + Y\mathrm{e}^{-\kappa z}) \times \sin(\hat{\alpha}x)\cos(\hat{\beta}y)\,\mathrm{d}\hat{\alpha}\,\mathrm{d}\hat{\beta}, \tag{11}$$

where X and Y are unknown functions of separation variables $\hat{\alpha}$ and $\hat{\beta}$, and $\kappa = (\hat{\alpha}^2 + \hat{\beta}^2)^{1/2}$. The second term on the right-hand side of Eq. (10), C_p, is a solution of Eq. (3) in spherical coordinates representing the disturbance generated by the spherical particle and is given by an infinite series in harmonics,

$$C_p = E_\infty \sum_{n=1}^{\infty} R_n r^{-n-1} P_n^1(\mu)\cos\phi, \tag{12}$$

where P_n^1 is the associated Legendre function of order n and degree one, μ is used to denote $\cos\theta$ for brevity, and R_n are unknown constants. Note that a solution for C of the form given by Eqs. (10)–(12) immediately satisfies the boundary condition at infinity in Eq. (8).

Substituting the solute concentration distribution C given by Eqs. (10)–(12) into the boundary conditions in Eq. (7) or Eq. (9) and applying the Fourier sine and cosine transforms on the variables x and y, respectively, lead to a solution for the functions X and Y in terms of the coefficients R_n. After the substitution of this solution into Eq. (11) and utilization of the integral representations of the modified Bessel functions of the second kind, the concentration distribution C can be expressed as

$$C = C_0 + E_\infty x + E_\infty \sum_{n=1}^{\infty} R_n \delta_n^{(1)}(r,\mu)\cos\phi, \tag{13}$$

where the function $\delta_n^{(1)}(r,\mu)$ is defined by Eq. (B.1) in Appendix B. Applying the boundary condition given by Eq. (4) to Eq. (13) yields

$$\sum_{n=1}^{\infty} R_n \left[\left(1 - \frac{2\beta}{a}\right)\delta_n^{(2)}(a,\mu) + \beta\delta_n^{(4)}(a,\mu)\right] = (1-\mu^2)^{1/2}, \tag{14}$$

where the definitions of functions $\delta_n^{(2)}(r,\mu)$ and $\delta_n^{(4)}(r,\mu)$ are given by Eqs. (B.2) and (B.4). Note that the definite integrals in $\delta_n^{(1)}$, $\delta_n^{(2)}$, and $\delta_n^{(4)}$ must be performed numerically.

To satisfy the condition in Eq. (14) exactly along the entire surface of the particle would require the solution of the entire infinite array of unknown constants R_n. However, the collocation method (O'Brien, 1968; Ganatos, Weinbaum, & Pfeffer, 1980; Keh & Jan, 1996) enforces the boundary condition at a finite number of discrete points on the half-circular generating arc of the sphere (from $\theta = 0$ to π) and truncates the infinite series in Eq. (13) into finite ones. If the spherical boundary is approximated by satisfying the condition of Eq. (4) at M discrete points on its generating arc, the infinite series in Eq. (13) is truncated after M terms, resulting in a system of M simultaneous linear algebraic equations in the truncated form of Eq. (14). This matrix equation can be numerically solved to yield the M unknown constants R_n required in the truncated form of Eq. (13) for the solute concentration distribution. The accuracy of the boundary-collocation/truncation technique can be improved to any degree by taking a sufficiently large value of M. Naturally, as $M \to \infty$ the truncation error vanishes and the overall accuracy of the solution depends only on the numerical integration required in evaluating the matrix elements.

2.2. Fluid velocity distribution

With knowledge of the solution for the solute concentration distribution on the particle surface which drives the migration, we can now proceed to find the flow field. The fluid solution is assumed to be incompressible and Newtonian. Owing to the low Reynolds number, the fluid motion in the outer region caused by the diffusiophoretic motion of the particle is governed by the Stokes equations,

$$\eta\nabla^2\mathbf{v} - \nabla p = \mathbf{0}, \tag{15a}$$

$$\nabla\cdot\mathbf{v} = 0, \tag{15b}$$

where $\mathbf{v}$ is the velocity field for the fluid flow and p is the dynamic pressure distribution.

The boundary conditions for the fluid velocity at the particle surface (Anderson & Prieve, 1991), on the plane walls, and far removed from the particle are

$$r = a: \quad \mathbf{v} = \mathbf{U} + a\boldsymbol{\Omega}\times\mathbf{e}_r - \frac{kT}{\eta}L^*K(\mathbf{e}_\theta\mathbf{e}_\theta + \mathbf{e}_\phi\mathbf{e}_\phi)\cdot\nabla C, \tag{16}$$

$$z = c,\ -b: \quad \mathbf{v} = \mathbf{0}, \tag{17}$$

$$\rho \to \infty: \quad \mathbf{v} = \mathbf{0}. \tag{18}$$

Here, $\mathbf{e}_r$, $\mathbf{e}_\theta$, and $\mathbf{e}_\phi$ are the unit vectors in spherical coordinates, and $\mathbf{U} = U\mathbf{e}_x$ and $\boldsymbol{\Omega} = \Omega\mathbf{e}_y$ are the translational and angular velocities of the particle undergoing diffusiophoresis to be determined. For the asymmetric problem as $b \neq c$, the assumption that the sphere would migrate in a direction parallel to the solute concentration gradient is justified in the absence of inertia. Note that the possible diffusioosmotic flow caused by the plane walls is ignored.

A fundamental solution to Eq. (15) which satisfies Eqs. (17) and (18) is

$$\mathbf{v} = v_x\mathbf{e}_x + v_y\mathbf{e}_y + v_z\mathbf{e}_z, \tag{19}$$

where

$$v_x = \sum_{n=1}^{\infty} [A_n(A_n' + \alpha_n') + B_n(B_n' + \beta_n') + C_n(C_n' + \gamma_n')], \quad (20a)$$

$$v_y = \sum_{n=1}^{\infty} [A_n(A_n'' + \alpha_n'') + B_n(B_n'' + \beta_n'') + C_n(C_n'' + \gamma_n'')], \quad (20b)$$

$$v_z = \sum_{n=1}^{\infty} [A_n(A_n''' + \alpha_n''') + B_n(B_n''' + \beta_n''') + C_n(C_n''' + \gamma_n''')]. \quad (20c)$$

Here, the primed A_n, B_n, C_n, α_n, β_n, and γ_n are functions of position involving associated Legendre functions of μ or $\cos\theta$ defined by Eq. (2.6) and in the form of integration (which must be performed numerically) defined by Eq. (C1) of Ganatos et al. (1980), and A_n, B_n, and C_n are unknown constants.

The boundary condition that remains to be satisfied is that on the particle surface. Substituting Eqs. (13) and (19) into Eq. (16), one obtains

$$\sum_{n=1}^{\infty} [A_n(A_n' + \alpha_n') + B_n(B_n' + \beta_n') + C_n(C_n' + \gamma_n')] = U - a\Omega\mu\cos\phi - U^{(0)}(H_1\mu\cos\phi + H_2\sin^2\phi), \quad (21a)$$

$$\sum_{n=1}^{\infty} [A_n(A_n'' + \alpha_n'') + B_n(B_n'' + \beta_n'') + C_n(C_n'' + \gamma_n'')] = -a\Omega\mu\sin\phi - U^{(0)}(H_1\mu\sin\phi - H_2\cos\phi\sin\phi), \quad (21b)$$

$$\sum_{n=1}^{\infty} [A_n(A_n''' + \alpha_n''') + B_n(B_n''' + \beta_n''') + C_n(C_n''' + \gamma_n''')] = a\Omega(1-\mu^2)^{1/2} + U^{(0)}H_1(1-\mu^2)^{1/2}, \quad (21c)$$

where

$$H_1 = \mu\cos\phi + \frac{1}{a}\sum_{n=1}^{\infty} R_n\delta_n^{(3)}(a,\mu), \quad (22a)$$

$$H_2 = 1 + \frac{1}{a(1-\mu^2)^{1/2}}\sum_{n=1}^{\infty} R_n\delta_n^{(1)}(a,\mu), \quad (22b)$$

$U^{(0)} = kTL^*KE_\infty/\eta$, and the function $\delta_n^{(3)}(r,\mu)$ is defined by Eq. (B.3). The first M coefficients R_n have been determined through the procedure given in the previous subsection.

Careful examination of Eqs. (21a)–(21c) shows that the solution of the coefficient matrix generated is independent of the ϕ coordinate of the boundary points on the surface of the sphere $r = a$. Thus, these relations can be satisfied by utilizing the collocation technique presented for the solution of the solute concentration field. At the particle surface, Eqs. (21a)–(21c) are applied at N discrete points (values of θ between 0 and π) and the infinite series in Eq. (20) are truncated after N terms. This generates a set of $3N$ linear algebraic equations for the $3N$ unknown coefficients A_n, B_n, and C_n. The fluid velocity field is completely obtained once these coefficients are solved for a sufficiently large value of N.

2.3. Derivation of the particle velocities

The drag force and torque exerted by the fluid on the spherical particle can be determined from (Ganatos et al., 1980)

$$\mathbf{F} = -8\pi\eta A_1\mathbf{e}_x, \quad (23a)$$

$$\mathbf{T} = -8\pi\eta C_1\mathbf{e}_y. \quad (23b)$$

These expressions show that only the lowest-order coefficients A_1 and C_1 in Eq. (20) contribute to the hydrodynamic force and couple acting on the particle.

Because the particle is freely suspended in the surrounding fluid, the net force and torque exerted on the particle must vanish. Applying this constraint to Eq. (23), one has

$$A_1 = C_1 = 0. \quad (24)$$

To determine the translational and angular velocities U and Ω of the particle, Eq. (24) and the $3N$ algebraic equations resulting from Eq. (21) are to be solved simultaneously.

3. Results and discussion

The solution for the diffusiophoretic motion of a spherical particle parallel to two plane walls at an arbitrary position between them, obtained by using the boundary collocation method described in the previous section, is presented in this section. The system of linear algebraic equations to be solved for the coefficients R_n is constructed from Eq. (14), while that for A_n, B_n, and C_n is composed of Eq. (21). All the numerical integrations to evaluate the primed α_n, β_n, and γ_n as well as $\delta_n^{(i)}$ functions were done by the 80-point Gauss–Laguerre guadrature. The numerical calculations were performed by using a DEC 3000/600 workstation.

When specifying the points along the semicircular generating arc of the sphere (with a constant value of ϕ) where the boundary conditions are to be exactly satisfied, the first points that should be chosen are $\theta = 0$ and π, since these points define the projected area of the particle normal to the direction of motion and control the gaps between the particle and the neighboring plates. In addition, the point $\theta = \pi/2$ is also important. However, an examination of the systems of linear algebraic equations (14) and (21) shows that the matrix equations become singular if these points are used.

Table 1
Normalized translational and rotational velocities of a spherical particle undergoing diffusiophoresis parallel to a single impermeable plane wall computed from the exact boundary-collocation solution and the asymptotic method-of-reflection solution

a/b	U/U_0			$-a\Omega/U_0$		
	Exact solution[a]		Asymptotic solution	Exact solution[a]		Asymptotic solution
$\beta/a = 0$						
0.2	0.99953	(0.99953)	0.99953	0.00030	(0.00030)	0.00031
0.4	0.99684	(0.99684)	0.99688	0.00492	(0.00492)	0.00540
0.6	0.99172	(0.99172)	0.99166	0.02669	(0.02669)	0.03455
0.8	0.98853	(0.98853)	0.98336	0.10164	(0.10164)	0.15360
0.9	0.99789	(0.99789)	0.97635	0.20389	(0.20389)	0.29818
0.95	1.0223	(1.02231)	0.97135	0.3189	(0.31890)	0.40846
0.99	1.1450	(1.14536)	0.96629	0.6162	(0.61832)	0.52144
0.995	1.230	(1.23060)		0.761	(0.76533)	
0.999	1.449			1.075		
$\beta/a = 10$						
0.2	0.99816		0.99816	0.00030		0.00030
0.4	0.98558		0.98563	0.00496		0.00483
0.6	0.95065		0.95099	0.02723		0.02484
0.8	0.87024		0.87445	0.10440		0.08088
0.9	0.78727		0.80822	0.20427		0.13233
0.95	0.7117		0.76452	0.3033		0.16632
0.99	0.5737		0.72318	0.4851		0.19826
0.995	0.536			0.538		
0.999	0.501			0.596		

[a]Values in parentheses were obtained by Keh and Chen (1988) using bipolar coordinates.

To overcome this difficulty, these points are replaced by closely adjacent points, i.e., $\theta=\delta$, $\pi/2-\delta$, $\pi/2+\delta$ and $\pi-\delta$ (Ganatos et al., 1980). Additional points along the boundary are selected as mirror-image pairs about the plane $\theta=\pi/2$ to divide the two quarter-circular arcs of the particle into equal segments. The optimum value of δ in this work is found to be 0.1°, with which the numerical results of the particle velocities converge satisfactorily. In selecting the boundary points, any value of ϕ may be used except for $\phi = 0,\ \pi/2$, and π since the matrix equation (21) is singular for these values.

3.1. Motion parallel to a single plane wall

The collocation solutions for the translational and rotational velocities of a spherical particle undergoing diffusiophoresis parallel to a plane wall (with $c \to \infty$) for different values of the relaxation parameter β/a and separation parameter a/b are presented in Tables 1 and 2 for the cases of an impermeable wall and a wall with the imposed far-field solute concentration gradient, respectively. The velocity for the diffusiophoretic motion of an identical particle in an infinite fluid, U_0, given by Eq. (2), is used to normalize the boundary-corrected values. All of the results obtained under the collocation scheme converge satisfactorily to at least the significant figures shown in the tables. The accuracy and convergence behavior of the truncation technique is principally a function of the ratio a/b. For the most difficult case with $a/b = 0.999$, the numbers of collocation points $M = 36$ and $N = 36$ are sufficiently large to achieve this convergence.

Through the use of spherical bipolar coordinates, Keh and Chen (1988) obtained semianalytical–seminumerical solutions for the normalized translational and rotational velocities of a dielectric sphere surrounded by an infinitesimally thin electric double layer undergoing electrophoresis parallel to a nonconducting plane wall. These solutions, which can apply to the case of diffusiophoresis of a sphere with $\beta/a = 0$ parallel to an impermeable plane wall, are also presented in Table 1 for comparison. It can be seen that our collocation solutions for the particle velocities agree excellently with the bipolar-coordinate solutions.

In Appendix A, an approximate analytical solution for the same diffusiophoretic motion as that considered here is also obtained by using a method of reflections. The translational and angular velocities of a spherical particle near a lateral plate are given by Eqs. (A.11a) and (A.11b), which are power series expansions in λ $(=a/b)$. The values of the wall-corrected normalized particle velocities calculated from this asymptotic solution, with the $O(\lambda^8)$ term neglected, are also listed in Tables 1 and 2 for comparison. It can be seen that the asymptotic formula of Eq. (A.11a) from the method of reflections for U/U_0 agrees very well with the exact results as long as $\lambda \leqslant 0.8$; the errors in all cases are less than 1.1%. However, the accuracy of Eqs. (A.11a) and (A.11b) [especially of Eq. (A.11b) for $a\Omega/U_0$, in which the leading term is $O(\lambda^4)$] deteriorates rapidly, as

Table 2
Normalized translational and rotational velocities of a spherical particle undergoing diffusiophoresis parallel to a single plane wall prescribed with the far-field solute concentration profile computed from the exact boundary-collocation solution and the asymptotic method-of-reflection solution

a/b	U/U_0		$-a\Omega/U_0$	
	Exact solution	Asymptotic solution	Exact solution	Asymptotic solution
$\beta/a = 0$				
0.2	0.99853	0.99853	0.00030	0.00030
0.4	0.98840	0.98846	0.00498	0.00480
0.6	0.95922	0.95993	0.02767	0.02422
0.8	0.88358	0.89274	0.10880	0.07619
0.9	0.79405	0.83125	0.21593	0.12162
0.95	0.7074	0.78952	0.3200	0.15067
0.99	0.5509	0.74938	0.4940	0.17738
0.995	0.510		0.539	
0.999	0.468		0.584	
$\beta/a = 10$				
0.2	0.99990	0.99990	0.00030	0.00030
0.4	0.99973	0.99977	0.00494	0.00536
0.6	1.00126	1.00132	0.02715	0.03393
0.8	1.00835	1.00571	0.10687	0.14890
0.9	1.01621	1.00762	0.22178	0.28746
0.95	1.0216	1.00774	0.3556	0.39282
0.99	1.0251	1.00708	0.6874	0.50057
0.995	1.036		0.826	
0.999	1.098		1.040	

expected, when the relative spacing between the particle and the plane wall becomes small.

The exact numerical solutions for the normalized velocities U/U_0 and $a\Omega/U_0$ of a spherical particle undergoing diffusiophoresis parallel to a plane wall as functions of a/b are depicted in Fig. 2 for various values of β/a. It can be seen that the wall-corrected normalized diffusiophoretic mobility U/U_0 of the particle decreases with an increase in β/a for the case of an impermeable wall (the boundary condition (7) is used), but increases with an increase in β/a for the case of a plane wall prescribed with the far-field solute concentration distribution (the boundary condition (9) is used), keeping the ratio a/b unchanged. This decrease and increase in the particle mobility becomes more pronounced as a/b increases. This behavior is expected knowing that the solute concentration gradients on the particle surface near an impermeable wall decrease as the relaxation parameter β/a increases and these gradients near a wall with the imposed far-field concentration gradient increase as β/a increases (see the analysis in Appendix A). When $\beta/a = 1/2$, the two types of plane wall will result in the same effects on the diffusiophoretic motion of the particle. In this particular case, the effect of solutal interaction between the particle and the wall disappears, and the relative diffusiophoretic mobility of the particle decreases monotonically with a/b solely owing to the hydrodynamic resistance exerted by the presence of the wall.

Examination of the results shown in Tables 1 and 2 and Fig. 2a reveals an interesting feature. For the case that the wall is an impermeable plane under the situation of small β/a (e.g., with $\beta/a = 0$), the diffusiophoretic mobility of the particle decreases with an increase in a/b as a/b is small, but increases from a minimum with increasing a/b as a/b is sufficiently large. When the gap between the particle and the wall turns thin, the particle can even move faster than it would at $a/b = 0$. For example, as $\beta/a = 0$ and $a/b = 0.999$, the diffusiophoretic velocity can be as much as 45% higher than the value with the wall being far away from the particle. Under the situation of relatively large β/a, the diffusiophoretic mobility of the particle near the impermeable wall is a monotonically decreasing function of a/b. For the case that a linear solute concentration profile is prescribed on the plane wall which is consistent with the far-field distribution under the situation of large β/a (e.g., with $\beta/a = 10$), the diffusiophoretic mobility of the particle first goes through a minimum with the increase of a/b from $a/b = 0$ and then increases monotonically. Again, the value of U/U_0 can be greater than unity when $a/b \to 1$. Under the situation of relatively small β/a, the diffusiophoretic mobility of the particle near the wall prescribed with the far-field solute concentration distribution becomes a monotonically decreasing function of a/b. This interesting feature that U/U_0 may not be a monotonic function of a/b and can even be greater than unity is understandable because the wall effect of hydrodynamic resistance on the particle is in competition with the wall effect of solutal enhancement when a particle with small β/a is undergoing diffusiophoretic motion parallel to an impermeable plate or when a particle with large β/a is

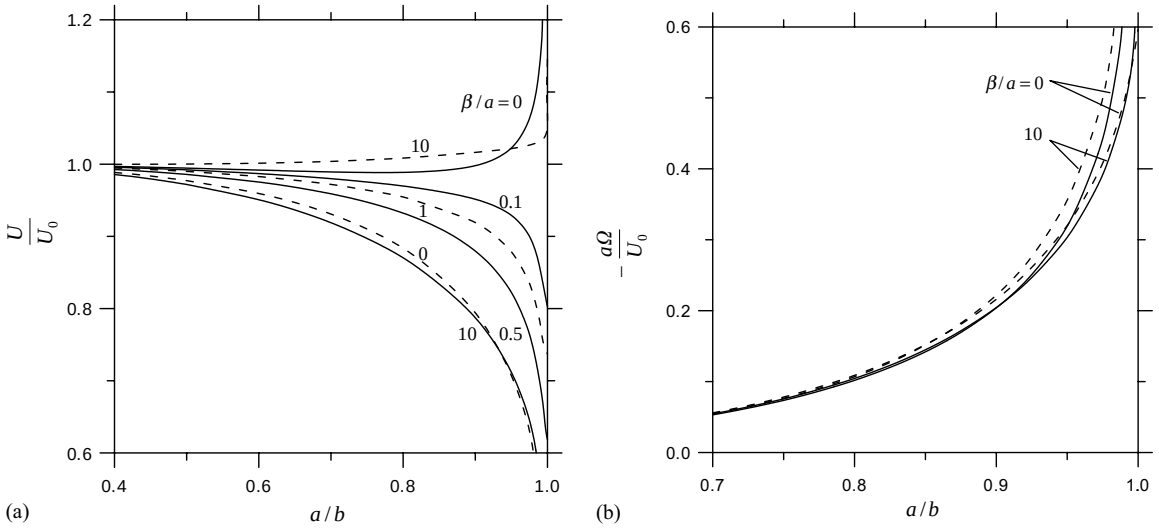

Fig. 2. Plots of the normalized velocities of a spherical particle undergoing diffusiophoresis parallel to a plane wall versus the separation parameter a/b for various values of β/a: (a) translational velocity U/U_0; (b) rotational velocity $a\Omega/U_0$. The solid curves represent the case of an impermeable wall, and the dashed curves denote the case of a wall on which the far-field solute concentration gradient is imposed.

moving near a lateral plate with the imposed far-field solute concentration gradient. A careful examination of the asymptotic formula for U/U_0 given by Eq. (A.11a) shows a good agreement of the numerical outcome in Fig. 2a with the analytical solution.

The results in Tables 1 and 2 and Fig. 2b indicate that the spherical particle undergoing diffusiophoresis parallel to a plane wall rotates in the direction opposite to that for a sphere migrating in the same direction but under a body-force field (e.g., a gravitational field). The explanation for this behavior is analogous to the case of electrophoresis of a charged sphere with a thin double layer parallel to a nonconducting plate (Keh & Chen, 1988). For any specified value of β/a, the magnitude of the normalized rotational velocity of the diffusiophoretic sphere near a given plane wall is a monotonically increasing function of a/b. For a fixed value of a/b not close to unity, the value of $a\Omega/U_0$ is not a sensitive function of β/a. On the other hand, for a given value of a/b close to unity, the value of $-a\Omega/U_0$ decreases with an increase in β/a for the diffusiophoresis parallel to an impermeable plate but increases with an increase in β/a for the migration parallel to a wall prescribed with the far-field solute concentration profile.

For the creeping motion of a spherical particle on which a constant body force $F\mathbf{e}_x$ is exerted parallel to an infinite plane wall, the exact result of the particle velocity has been developed by using a method of spherical bipolar coordinates (O'Neill, 1964) and the boundary-collocation technique (Ganatos et al., 1980). A comparison of the boundary effects on the translation of the sphere under gravity (in which $U_0 = F/6\pi\eta a$) and on the diffusiophoresis indicates that the wall effect on diffusiophoretic motion is much weaker than that on a sedimenting particle.

3.2. Motion parallel to two plane walls

The converged collocation solutions for the normalized velocity U/U_0 of a spherical particle undergoing diffusiophoresis on the median plane between two parallel plane walls (with $c = b$ and $\Omega = 0$) for various values of the parameters β/a and a/b are presented in Table 3 for both cases of impermeable walls and walls prescribed with the far-field solute concentration distribution. The corresponding method-of-reflection solutions, given by Eq. (A.20) in Appendix A as a power series expansion in λ $(=a/b)$ correct to $O(\lambda^7)$, are also listed in this table for comparison. Similar to the case of migration of a spherical particle parallel to a single plane wall considered in the previous subsection, the approximate analytical formula of Eq. (A.20) agrees very well with the exact results as long as $\lambda \leqslant 0.6$, but can have significant errors when $\lambda \geqslant 0.8$. In general, Eq. (A.20) overestimates the diffusiophoretic velocity of the particle. A comparison between Table 3 for the case of a slit and Tables 1 and 2 for the case of a single parallel plane indicates that the assumption that the boundary effect for two walls can be obtained by simple addition of single-wall effects leads to a smaller correction to diffusiophoretic motion as a/b is small but can give a greater correction as a/b becomes large.

In Fig. 3, the collocation results for the normalized diffusiophoretic mobility U/U_0 of a sphere migrating on the median plane between two parallel plane walls are plotted as functions of a/b for several values of β/a. Analogous to the corresponding motion of a particle parallel to a single plane wall, for a specified value of a/b, U/U_0 increases with an increase in β/a for the case of walls with the imposed far-field solute concentration gradient and decreases with an increase in β/a for the case of impermeable walls. Again, for

Table 3
Normalized diffusiophoretic velocity of a spherical particle along the median plane between two parallel plane walls computed from the exact boundary-collocation solution and the asymptotic method-of-reflection solution

a/b	U/U_0			
	$\beta/a = 0$		$\beta/a = 10$	
	Exact solution	Asymptotic solution	Exact solution	Asymptotic solution
For impermeable plane walls				
0.2	0.99796	0.99796	0.99470	0.99470
0.4	0.98597	0.98617	0.96038	0.96083
0.6	0.96339	0.96661	0.87952	0.88817
0.8	0.94684	0.96326	0.74486	0.81008
0.9	0.96662	0.98325	0.64927	0.79933
0.95	1.0163	1.00270	0.5839	0.81018
0.99	1.2243	1.02412	0.4935	0.82992
0.995	1.363		0.481	
0.999	1.718		0.494	
For plane walls prescribed with the far-field concentration profile				
0.2	0.99586	0.99587	0.99832	0.99832
0.4	0.96931	0.96975	0.98877	0.98899
0.6	0.90602	0.91448	0.97215	0.97605
0.8	0.79069	0.85485	0.96200	0.98514
0.9	0.69390	0.84471	0.97401	1.01389
0.95	0.6184	0.85078	0.9974	1.03838
0.99	0.5075	0.86316	1.0550	1.06415
0.995	0.490		1.113	
0.999	0.497		1.256	

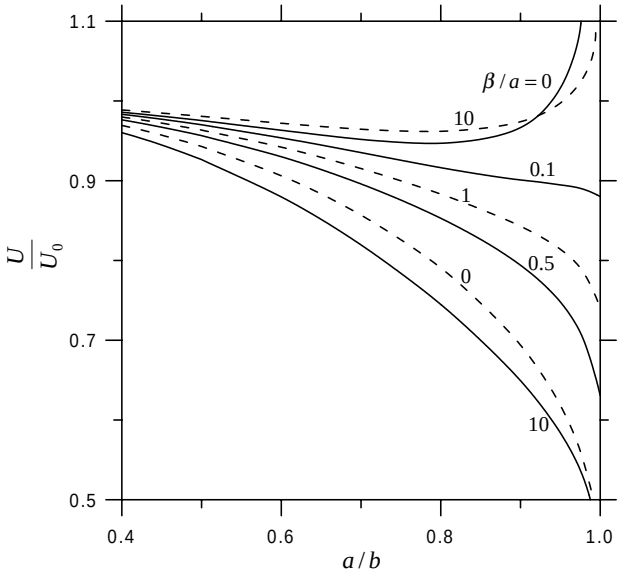

Fig. 3. Plots of the normalized diffusiophoretic mobility U/U_0 of a spherical particle migrating on the median plane between two parallel plane walls (with $c = b$) versus the separation parameter a/b for several values of β/a. The solid curves represent the case of impermeable walls, and the dashed curves denote the case of walls prescribed with the far-field solute concentration distribution.

the case of impermeable walls under the situation of small β/a, or for the case of walls prescribed with the far-field solute concentration distribution under the situation of large β/a, the diffusiophoretic mobility of the particle first goes through a minimum with the increase of a/b from $a/b = 0$ and then increases monotonically, and the particle can even move faster than it would at $a/b = 0$. This result indicates that the effect of solutal enhancement, rather than that of hydrodynamic resistance, can be overriding when the particle–wall gap thickness is small. An examination of the asymptotic formula for U/U_0 in Eq. (A.20) also shows a good agreement of the trend in Fig. 3 with the analytical solution.

A careful comparison of the curves in Fig. 3 for the case of a slit with the corresponding curves in Fig. 2a for the case of a single wall reveals an interesting feature of the boundary effect on diffusiophoresis of a colloidal sphere. The presence of a second, identical, lateral plane wall, even at a symmetric position with respect to the sphere against the first, does not always enhance the wall effect on the diffusiophoretic particle induced by the first plate only. This result reflects again the fact that the lateral wall can affect the solutal driving force and the viscous drag force on a particle in opposite directions. Each force is increased in its own direction as the value of a/b turns small, but to a different degree, for the case of diffusiophoretic motion of a particle in a slit relative to that for the case of migration parallel to a single plate. Thus, the net effect composed of these two opposite forces for the slit case is not necessarily to enhance that for the case of a single wall.

Fig. 4 shows the collocation results for the normalized translational velocity U/U_0 and rotational velocity $a\Omega/U_0$

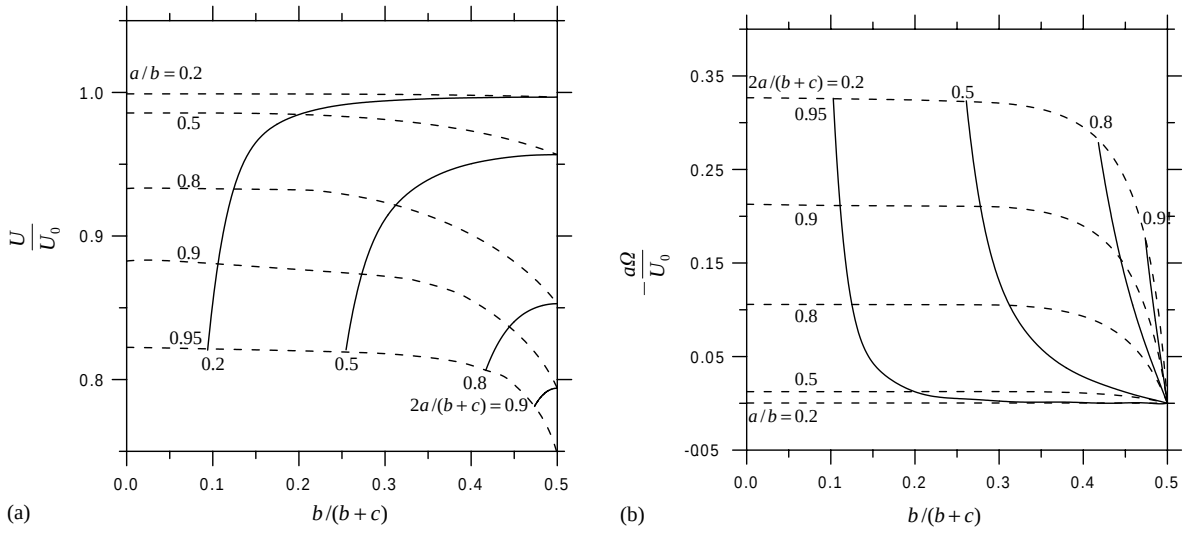

Fig. 4. Plots of the normalized velocities of a spherical particle undergoing diffusiophoresis parallel to two plane walls versus the ratio $b/(b+c)$ for the case of $\beta/a = 1/2$ with a/b and $2a/(b+c)$ as parameters: (a) translational velocity U/U_0; (b) rotational velocity $a\Omega/U_0$.

of a colloidal sphere undergoing diffusiophoresis parallel to two plane walls at various positions between them for a typical case with $\beta/a = 1/2$ (the results for the two types of plane walls are identical in this case). The dashed curves (with $a/b =$ constant) illustrate the effect of the position of the second wall (at $z = c$) on the particle velocities for various values of the relative sphere-to-first-wall spacing b/a. The solid curves (with $2a/(b+c) =$ constant) indicate the variation of the particle velocities as functions of the sphere position at various values of the relative wall-to-wall spacing $(b+c)/2a$. As illustrated in Fig. 4a, the net wall effect for the given case is to reduce the diffusiophoretic mobility U/U_0 of the particle. At a constant value of $2a/(b+c)$, the particle experiences a minimum viscous drag force and has a greatest translational velocity (without rotation) when it is located midway between the two walls (with $c = b$). The hydrodynamic drag increases, the translational velocity decreases, and the rotational velocity increases as the particle approaches either of the walls (or the ratio $b/(b+c)$ decreases). At a specified value of a/b for the diffusiophoretic particle near a first lateral wall, the presence of a second plate is to further reduce the translational and rotational velocities of the particle, and the degree of this reduction increases monotonically with a decrease in the relative distance between the particle and the second plate (or with an increase in $b/(b+c)$).

On the other hand, for some cases such as the diffusiophoresis of a colloidal sphere with a small value of β/a parallel to two impermeable plane walls or with a large value of β/a parallel to two plates prescribed with the far-field solute concentration distribution, the net wall effect can increase the diffusiophoretic mobility of the particle relative to its isolated value. At a fixed value of $2a/(b+c)$ in these cases, the normalized particle mobility has a relatively small value as it is located midway between the two walls, where the particle experiences a minimum effect of solutal enhancement, and becomes relatively large when it approaches either of the walls. At a given value of a/b for the diffusiophoretic particle and the first lateral plate, the effect induced by the presence of the second plate on the particle mobility is not necessarily a monotonic function of its distance from the particle. This dependence is not graphically presented here for conciseness.

The collocation solution for the problem of sedimentation of a sphere parallel to two plane walls at an arbitrary position between them was also obtained (Ganatos et al., 1980). Comparing that solution with the present results, we still find that the wall effect on diffusiophoresis in general is much weaker than that on sedimentation.

4. Conclusions

In this work, the exact numerical solutions and approximate analytical solutions for the quasisteady diffusiophoretic motion of a colloidal sphere parallel to two infinite plane walls at an arbitrary position between them have been obtained by using the boundary-collocation technique and the method of reflections, respectively. Both the cases of impermeable walls and of walls with the imposed far-field solute concentration gradient were examined in the limit of vanishingly small Reynolds and Peclet numbers. It has been found that the boundary effect on diffusiophoretic motion of a particle is quite complicated. The diffusiophoretic mobility of a particle near a wall is generally, but not necessarily, a monotonic decreasing function of the separation parameter a/b. When the value of a/b is close to unity, the effect of a lateral wall can speed up or slow down the particle

velocity relative to its isolated value depending on the value of the relaxation parameter β/a of the particle and the solutal boundary condition at the wall. This behavior reflects the competition between the relatively weak hydrodynamic retardation exerted by the neighboring wall on the particle migration and the possible, strong diffusiophoretic enhancement due to the solutal interaction between the particle and the lateral wall.

Notation

a	radius of the particle, m
A	diffusiophoretic mobility defined by Eq. (2b), $m^5\ s^{-1}$
A_n, B_n, C_n	coefficients in Eq. (20) for the flow field, $m^{n+1}\ s^{-1}$, $m^{n+3}\ s^{-1}$, $m^{n+2}\ s^{-1}$
b, c	the respective distances from the particle center to the two plates, m
C	solute concentration field in the fluid, m^{-3}
C_∞	prescribed solute concentration field defined by Eq. (8), m^{-3}
$\mathbf{e}_x, \mathbf{e}_y, \mathbf{e}_z$	unit vectors in rectangular coordinates
$\mathbf{e}_r, \mathbf{e}_\theta, \mathbf{e}_\phi$	unit vectors in spherical coordinates
E_∞	$=\lvert\nabla C_\infty\rvert$, m^{-4}
G	dimensionless parameter defined right after Eq. (A.4)
k	Boltzmann's constant, $J\ K^{-1}$
K	Gibbs adsorption length defined by Eq. (6b), m
L^*	characteristic length for the particle–solute interaction defined by Eq. (6c), m
r	radial spherical coordinate, m
R_n	coefficients in Eqs. (12) and (13) for the solute concentration field, m^{n+2}
T	absolute temperature, K
$\mathbf{U}, U$	translational velocity of the particle, $m\ s^{-1}$
$\mathbf{U}_0, U_0$	diffusiophoretic velocity of an isolated particle defined by Eq. (2), $m\ s^{-1}$
$\mathbf{v}$	velocity field of the fluid, $m\ s^{-1}$
x, y, z	rectangular coordinates, m

Greek letters

β	relaxation coefficient defined by Eq. (5), m
$\delta_n^{(1)}, \delta_n^{(2)}, \delta_n^{(3)}, \delta_n^{(4)}$	functions of r and μ defined by Eqs. (B.1)–(B.4), m^{-n-1}, m^{-n-2}, m^{-n-1}, m^{-n-3}
η	viscosity of the fluid, $kg\ m^{-1}\ s^{-1}$
θ, ϕ	angular spherical coordinates
λ	$=a/b$
μ	$=\cos\theta$
ρ	radial cylindrical coordinate, m
$\mathbf{\Omega}, \Omega$	angular velocity of the particle, s^{-1}

Subscripts

p	particle
w	wall

Acknowledgements

This research was partly supported by the National Science Council of the Republic of China.

Appendix A. Analysis of the diffusiophoresis of a spherical particle parallel to one or two plane walls by a method of reflections

In this appendix, we analyze the quasisteady diffusiophoretic motion of a colloidal sphere either parallel to an infinite flat wall ($c \to \infty$) or on the median plane between two parallel plates ($c = b$), as shown in Fig. 1, by a method of reflections. The effect of the walls on the translational velocity $\mathbf{U}$ and angular velocity $\mathbf{\Omega}$ of the particle is sought in expansions of λ, which equals a/b, the ratio of the particle radius to the distance between the wall and the center of the particle.

A.1. Motion parallel to an infinite plane wall

For the problem of diffusiophoretic motion of a spherical particle parallel to an impermeable plane wall, the governing equations (3) and (15) must be solved by satisfying the boundary conditions (4), (7), (8), and (16)–(18) with $c \to \infty$. The method-of-reflection solution consists of the following series, whose terms depend on increasing powers of λ:

$$C = C_0 + E_\infty x + C_p^{(1)} + C_w^{(1)} + C_p^{(2)} + C_w^{(2)} + \cdots, \quad \text{(A.1a)}$$

$$\mathbf{v} = \mathbf{v}_p^{(1)} + \mathbf{v}_w^{(1)} + \mathbf{v}_p^{(2)} + \mathbf{v}_w^{(2)} + \cdots, \quad \text{(A.1b)}$$

where subscripts p and w represent the reflections from particle and wall, respectively, and the superscript (i) denotes the ith reflection from that surface. In these series, all the expansion sets of the corresponding concentration and velocity fields for the fluid solution must satisfy Eqs. (3) and (15). The advantage of this method is that it is necessary to consider boundary conditions associated with only one surface at a time.

According to Eq. (A.1), the translational and angular velocities of the particle can also be expressed in the series form,

$$\mathbf{U} = U_0 \mathbf{e}_x + \mathbf{U}^{(1)} + \mathbf{U}^{(2)} + \cdots, \quad \text{(A.2a)}$$

$$\mathbf{\Omega} = \mathbf{\Omega}^{(1)} + \mathbf{\Omega}^{(2)} + \cdots. \quad \text{(A.2b)}$$

In these expressions, $U_0 = AE_\infty$ is the diffusiophoretic velocity of an identical particle suspended freely in the continuous phase far from the wall given by Eq. (2); $\mathbf{U}^{(i)}$ and $\mathbf{\Omega}^{(i)}$ are related to $\nabla C_w^{(i)}$ and $\mathbf{v}_w^{(i)}$ by (Keh & Luo, 1995)

$$\mathbf{U}^{(i)} = A[\nabla C_w^{(i)}]_0 + [\mathbf{v}_w^{(i)}]_0 + \frac{a^2}{6}[\nabla^2 \mathbf{v}_w^{(i)}]_0, \quad \text{(A.3a)}$$

$$\mathbf{\Omega}^{(i)} = \frac{1}{2}[\nabla \times \mathbf{v}_w^{(i)}]_0, \quad \text{(A.3b)}$$

where the subscript 0 to variables inside brackets denotes evaluation at the position of the particle center.

The solution for the first reflected fields from the particle is

$$C_p^{(1)} = GE_\infty a^3 r^{-2} \sin\theta\cos\phi, \tag{A.4a}$$

$$\mathbf{v}_p^{(1)} = \tfrac{1}{2} U_0 a^3 r^{-3}(2\sin\theta\cos\phi\,\mathbf{e}_r - \cos\theta\cos\phi\,\mathbf{e}_\theta + \sin\phi\,\mathbf{e}_\phi), \tag{A.4b}$$

where $G = (1/2 - \beta/a)(1+\beta/a)^{-1}$. Obviously, $-1 \leqslant G \leqslant 1/2$, with the upper and lower bounds occurring at the limits $\beta/a = 0$ and $\beta/a \to \infty$, respectively. The velocity distribution shown in Eq. (A.4b) is identical to the irrotational flow surrounding a rigid sphere moving with velocity $U_0\mathbf{e}_x$.

The boundary conditions for the ith reflected fields from the wall are derived from Eqs. (7), (8), (17), and (18),

$$z = -b: \quad \frac{\partial C_w^{(i)}}{\partial z} = -\frac{\partial C_p^{(i)}}{\partial z}, \tag{A.5a}$$

$$\mathbf{v}_w^{(i)} = -\mathbf{v}_p^{(i)}; \tag{A.5b}$$

$$r \to \infty,\ z > -b: \quad C_w^{(i)} \to 0, \tag{A.5c}$$

$$\mathbf{v}_w^{(i)} \to \mathbf{0}. \tag{A.5d}$$

The solution of $C_w^{(1)}$ is obtained by applying complex Fourier transforms on x and y in Eqs. (3) and (A.5a) and (A.5c), with the result

$$C_w^{(1)} = GE_\infty a^3 x[x^2 + y^2 + (z+2b)^2]^{-3/2}. \tag{A.6a}$$

This reflected concentration field may be interpreted as arising from the reflection of the imposed field $E_\infty\mathbf{e}_x$ from a fictitious particle identical to the actual particle, its location being at the mirror-image position of the actual particle with respect to the plane $z = -b$ (i.e. at $x = 0,\ y = 0,\ z = -2b$). The solution for $\mathbf{v}_w^{(1)}$ can be found by fitting the boundary conditions (A.5b) and (A.5d) with the general solution to Eq. (15) established by Faxen (Happel & Brenner, 1983, p. 323), which results in

$$\mathbf{v}_w^{(1)} = \frac{U_0 a^3}{4\pi}\int_{-\infty}^{\infty}\int_{-\infty}^{\infty} \mathbf{e}^{\mathrm{i}(\hat\alpha x + \hat\beta y) - \kappa(z+2b)} \times \left\{ -[2\kappa(z+b)+1]\mathrm{i}\hat\alpha\mathbf{e}_z - [2\kappa(z+b)-1] \times \left(\frac{\hat\alpha^2}{\kappa}\mathbf{e}_x + \frac{\hat\alpha\hat\beta}{\kappa}\mathbf{e}_y\right)\right\} \mathrm{d}\hat\alpha\,\mathrm{d}\hat\beta, \tag{A.6b}$$

where $\kappa = (\hat\alpha^2 + \hat\beta^2)^{1/2}$ and $\mathrm{i} = \sqrt{-1}$.

The contributions of $C_w^{(1)}$ and $\mathbf{v}_w^{(1)}$ to the translational and angular velocities of the particle are determined by using Eq. (A.3),

$$\mathbf{U}_s^{(1)} = A[\nabla C_w^{(1)}]_{r=0} = \frac{1}{8} G\lambda^3 U_0\mathbf{e}_x, \tag{A.7a}$$

$$\mathbf{U}_h^{(1)} = \left[\mathbf{v}_w^{(1)} + \frac{a^2}{6}\nabla^2\mathbf{v}_w^{(1)}\right]_{r=0} = -\frac{1}{8}(\lambda^3 - \lambda^5)U_0\mathbf{e}_x, \tag{A.7b}$$

$$\mathbf{U}^{(1)} = \mathbf{U}_s^{(1)} + \mathbf{U}_h^{(1)} = \frac{1}{8}[-(1-G)\lambda^3 + \lambda^5]U_0\mathbf{e}_x, \tag{A.7c}$$

$$a\boldsymbol{\Omega}^{(1)} = \frac{a}{2}[\nabla\times\mathbf{v}_w^{(1)}]_{r=0} = -\frac{3}{16}U_0\lambda^4\mathbf{e}_y. \tag{A.7d}$$

Eq. (A.7a) shows that the reflected concentration field from the impermeable wall can increase (if $G > 0$ or $\beta/a < 1/2$) or decrease (if $G < 0$ or $\beta/a > 1/2$) the velocity of the diffusiophoretic particle, while Eq. (A.7b) indicates that the reflected velocity field is to decrease this velocity; the net effect of the reflected fields is expressed by Eq. (A.7c), which can enhance or retard the movement of the particle, depending on the combination of the values of G (or β/a) and λ. When $G = 0$ (or $\beta/a = 1/2$), the reflected solute concentration field makes no contribution to the diffusiophoretic velocity. Eq. (A.7c) indicates that the wall correction to the translational velocity of the diffusiophoretic particle is $\mathrm{O}(\lambda^3)$, which is weaker than that obtained for the corresponding sedimentation problem, in which the leading boundary effect is $\mathrm{O}(\lambda)$. Note that the necessary condition for the wall enhancement on the diffusiophoretic motion to occur is a small value of β/a and a value of λ close to unity such that the relation $\lambda^5 > (1-G)\lambda^3$ is warranted.

Eq. (A.7d) shows that the diffusiophoretic sphere rotates about an axis which is perpendicular to the direction of applied gradient and parallel to the plane wall. The direction of rotation is opposite to that which would occur if the sphere were driven to move by a body force. Note that the angular velocity $\boldsymbol{\Omega}^{(1)}$ in Eq. (A.7d) does not depend on the parameter G (since $\mathbf{v}_w^{(1)}$ is not a function of G). Also, the wall-induced angular velocity of the diffusiophoretic particle is $\mathrm{O}(\lambda^4)$, which is the same in order as but different in its coefficient ($-3/16$ versus $3/32$) from that of a rigid sphere moving under a body-force field (Happel & Brenner, 1983, p. 327).

The solution for the second reflected fields from the particle is

$$C_p^{(2)} = \frac{1}{8}E_\infty[G^2\lambda^3 a^3 r^{-2}\sin\theta\cos\phi + GH\lambda^4 a^4 r^{-3}\cos\theta\sin\theta\cos\phi + \mathrm{O}(\lambda^5 a^5)], \tag{A.8a}$$

$$\mathbf{v}_p^{(2)} = \frac{1}{32}U_0[2G\lambda^3 a^3 r^{-3}(2\sin\theta\cos\phi\,\mathbf{e}_r - \cos\theta\cos\phi\,\mathbf{e}_\theta + \sin\phi\,\mathbf{e}_\phi) + 9\left(4G\frac{B}{A} + 5\right)\lambda^4 a^2 r^{-2}\cos\theta\sin\theta\cos\phi\,\mathbf{e}_r - \frac{3}{16}\lambda^4 a^2 r^{-2}(\cos\phi\,\mathbf{e}_\theta - \cos\theta\sin\phi\,\mathbf{e}_\phi) + \mathrm{O}(\lambda^4 a^4, \lambda^5 a^3)]. \tag{A.8b}$$

Here, $H = 3(1-2\beta/a)(3+4\beta/a)^{-1}$ and $B = -(5kT/6\eta)L^* K(1+2\beta/a)^{-1}$.

The boundary conditions for the second reflected fields from the wall are obtained by substituting the results of $C_p^{(2)}$

and $\mathbf{v}_p^{(2)}$ into Eq. (A.5), with which Eqs. (3) and (15) can be solved as before to yield

$$[\nabla C_w^{(2)}]_{r=0} = \left[\frac{1}{64}\,G^2\lambda^6 + \mathrm{O}(\lambda^8)\right] E_\infty \mathbf{e}_x, \tag{A.9a}$$

$$[\mathbf{v}_w^{(2)}]_{r=0} = \left\{-\frac{1}{256}\left[4G\left(1+9\frac{B}{A}\right)+39\right]\lambda^6 + \mathrm{O}(\lambda^8)\right\} U_0\mathbf{e}_x. \tag{A.9b}$$

The contribution of the second reflected fields to the translational and angular velocities of the particle is obtained by putting $C_w^{(2)}$ and $\mathbf{v}_w^{(2)}$ into Eq. (A.3), which gives

$$\mathbf{U}^{(2)} = \left\{\frac{1}{256}\left[4G^2 - 4G\left(1+9\,\frac{B}{A}\right)-39\right]\lambda^6 + \mathrm{O}(\lambda^8)\right\} U_0\mathbf{e}_x, \tag{A.10a}$$

$$a\boldsymbol{\Omega}^{(2)} = \left\{\left[\frac{3}{256}\,G\left(1+39\frac{B}{A}\right)-\frac{93}{512}\right]\lambda^7 + \mathrm{O}(\lambda^9)\right\} U_0\mathbf{e}_y. \tag{A.10b}$$

The errors for $\mathbf{U}^{(2)}$ and $a\boldsymbol{\Omega}^{(2)}$ are $\mathrm{O}(\lambda^8)$ and $\mathrm{O}(\lambda^9)$, respectively, because the $\mathrm{O}(\lambda^7)$ terms in the expansions of $\nabla C_w^{(2)}$ and $\mathbf{v}_w^{(2)}$ vanish at the position of the particle center.

Obviously, $\mathbf{U}^{(3)}$ and $a\boldsymbol{\Omega}$ will be $\mathrm{O}(\lambda^9)$ and $\mathrm{O}(\lambda^{10})$, respectively. With the substitution of Eqs. (A.7c), (A.7d) and (A.10) into Eq. (A.2), the particle velocities can be expressed as $\mathbf{U} = U\mathbf{e}_x$ and $\boldsymbol{\Omega} = \Omega\mathbf{e}_y$ with

$$U = U_0\left\{1 - \frac{1}{8}\,(1-G)\lambda^3 + \frac{1}{8}\,\lambda^5 + \frac{1}{256}\left[4G^2 - 4\left(1+9\,\frac{B}{A}\right)G - 39\right]\lambda^6 + \mathrm{O}(\lambda^8)\right\}, \tag{A.11a}$$

$$a\Omega = U_0\left\{-\frac{3}{16}\,\lambda^4 + \left[\frac{3}{256}\,G\left(1+39\frac{B}{A}\right)-\frac{93}{512}\right]\lambda^7 + \mathrm{O}(\lambda^9)\right\}. \tag{A.11b}$$

The particle migrates along the imposed solute concentration gradient at a rate that can increase or decrease as the particle approaches the wall. Owing to the neglect of inertial effects, the wall does not deflect the direction of diffusiophoresis.

For the case that a linear solute concentration profile is prescribed on the plane wall which is consistent with the far-field distribution, namely, the boundary condition (7) is replaced by Eq. (9), the series expansions (A.1) and (A.2), the solutions of $C_p^{(1)}$ and $\mathbf{v}_p^{(1)}$ in Eq. (A.4), and the boundary conditions for $C_w^{(i)}$ and $\mathbf{v}_w^{(i)}$ in Eqs. (A.5b)–(A.5d) are still valid, while Eq. (A.5a) becomes

$$z = -b: \quad C_w^{(i)} = -C_p^{(i)}. \tag{A.12}$$

With this change, it can be shown that the results of the reflected fields and of the particle velocities are also obtained from Eqs. (A.6)–(A.11) by replacing G by $-G$. Thus, contrary to the effect of an impermeable plane wall, the reflected solute concentration field from a parallel wall with the imposed far-field concentration gradient reduces the translational velocity of the particle if $G > 0$ or $\beta/a < 1/2$ and enhances this velocity if $G < 0$ or $\beta/a > 1/2$. When $G = 0$ or $\beta/a = 1/2$, the two types of plane wall will produce the same effects on the diffusiophoretic motion of the particle. Under the conditions that the values of β/a and λ are sufficiently large such that $\lambda^5 > (1+G)\lambda^3$, the net effect of a lateral plane wall prescribed with the far-field concentration distribution can enhance the diffusiophoretic migration of a particle.

A.2. Motion on the median plane between two parallel flat walls

For the problem of diffusiophoretic motion of a sphere on the median plane between two impermeable parallel plates, the boundary conditions corresponding to governing equations (3) and (15) are given by Eqs. (4), (7), (8), and (16)–(18) with $c = b$. But, the angular velocity $\boldsymbol{\Omega}$ of the particle vanishes now because of the symmetry. With $\lambda = a/b \ll 1$, the series expansions of the solute concentration, fluid velocity, and particle velocity given by Eqs. (A.1), (A.2a), and (A.4) remain valid here. From Eqs. (7), (8), (17), and (18), the boundary conditions for $C_w^{(i)}$ and $\mathbf{v}_w^{(i)}$ are found to be

$$|z| = b: \quad \frac{\partial C_w^{(i)}}{\partial z} = -\frac{\partial C_p^{(i)}}{\partial z}, \tag{A.13a}$$

$$\mathbf{v}_w^{(i)} = -\mathbf{v}_p^{(i)}; \tag{A.13b}$$

$$r \to \infty,\ |z| \leqslant b: \quad C_w^{(i)} \to 0, \tag{A.13c}$$

$$\mathbf{v}_w^{(i)} \to \mathbf{0}. \tag{A.13d}$$

The first wall-reflected fields can be solved by the same method as used for a single lateral plate in the previous subsection, with the results

$$C_w^{(1)} = -\frac{GE_\infty a^3}{2\pi}\int_{-\infty}^{\infty}\int_{-\infty}^{\infty}\frac{\mathrm{i}\alpha}{\kappa}\,\mathrm{e}^{\mathrm{i}(\hat{\alpha}x+\hat{\beta}y)-\kappa b} \times \frac{\cosh(\kappa z)}{\sinh(\kappa b)}\,\mathrm{d}\hat{\alpha}\,\mathrm{d}\hat{\beta}, \tag{A.14a}$$

$$\mathbf{v}_w^{(1)} = \frac{U_0 a^3}{2\pi}\int_{-\infty}^{\infty}\int_{-\infty}^{\infty}\frac{1}{\sinh(2\kappa b)-2\kappa b}\mathrm{e}^{\mathrm{i}(\hat{\alpha}x+\hat{\beta}y)} \times \left\{[\sinh(\kappa z)-\kappa z\cosh(\kappa z)+g\sinh(\kappa z)]\mathrm{i}\hat{\alpha}\mathbf{e}_z + [\kappa z\sinh(\kappa z)-g\cosh(\kappa z)] \times \left(\frac{\hat{\alpha}^2}{\kappa}\,\mathbf{e}_x + \frac{\hat{\alpha}\hat{\beta}}{\kappa}\,\mathbf{e}_y\right)\right\}\mathrm{d}\hat{\alpha}\,\mathrm{d}\hat{\beta}, \tag{A.14b}$$

where $\kappa = (\hat{\alpha}^2 + \hat{\beta}^2)^{1/2}$ and $g = \kappa b - e^{-\kappa b}\sinh(\kappa b)$. The contributions of $C_w^{(1)}$ and $\mathbf{v}_w^{(1)}$ to the particle velocity are determined using Eq. (A.3a), which lead to a result similar to Eqs. (A.7a)–(A.7c),

$$\mathbf{U}_s^{(1)} = d_1 G\lambda^3 U_0 \mathbf{e}_x, \tag{A.15a}$$

$$\mathbf{U}_h^{(1)} = -(d_2\lambda^3 - d_3\lambda^5)U_0\mathbf{e}_x, \tag{A.15b}$$

$$\mathbf{U}^{(1)} = \mathbf{U}_s^{(1)} + \mathbf{U}_h^{(1)} = [-(d_2 - d_1 G)\lambda^3 + d_3\lambda^5]U_0\mathbf{e}_x, \tag{A.15c}$$

where

$$d_1 = \int_0^\infty \frac{\rho^2}{e^{2\rho}-1}\,d\rho = 0.300514, \tag{A.16a}$$

$$d_2 = \frac{1}{2}\int_0^\infty \frac{\rho^2(\rho - e^{-\rho}\sinh\rho)}{\sinh(2\rho) - 2\rho}\,d\rho = 0.417956, \tag{A.16b}$$

$$d_3 = \frac{1}{6}\int_0^\infty \frac{\rho^4}{\sinh(2\rho) - 2\rho}\,d\rho = 0.338324. \tag{A.16c}$$

Analogous to the previous case, the results of the second reflections can be obtained as

$$C_p^{(2)} = E_\infty[d_1 G^2\lambda^3 a^3 r^{-2}\sin\theta\cos\phi + O(\lambda^5 a^5)], \tag{A.17a}$$

$$\mathbf{v}_p^{(2)} = \frac{U_0}{2}[d_1 G\lambda^3 a^3 r^{-3}(2\sin\theta\cos\phi\mathbf{e}_r - \cos\theta\cos\phi\mathbf{e}_\theta + \sin\phi\mathbf{e}_\phi) + O(\lambda^5 a^3)], \tag{A.17b}$$

$$[\nabla C_w^{(2)}]_{r=0} = [d_1^2 G^2\lambda^6 + O(\lambda^8)]E_\infty\mathbf{e}_x, \tag{A.18a}$$

$$[\mathbf{v}_w^{(2)}]_{r=0} = [-d_1 d_2 G\lambda^6 + O(\lambda^8)]U_0\mathbf{e}_x \tag{A.18b}$$

and

$$\mathbf{U}^{(2)} = [-(d_1 d_2 G - d_1^2 G^2)\lambda^6 + O(\lambda^8)]U_0\mathbf{e}_x. \tag{A.19}$$

Note that the $\lambda^4 a^2$ and $\lambda^4 a^4$ terms in the expressions for $C_p^{(2)}$ and $\mathbf{v}_p^{(2)}$ vanish. With the combination of Eqs. (A.2a), (A.15c), and (A.19), the particle velocity can be expressed as $\mathbf{U} = U\mathbf{e}_x$ with

$$U = U_0[1 - (d_2 - d_1 G)\lambda^3 + d_3\lambda^5 - (d_1 d_2 G - d_1^2 G^2)\lambda^6 + O(\lambda^8)]. \tag{A.20}$$

For the case that the particle is undergoing diffusiophoresis on the median plane between two parallel plates on which a linear solute concentration profile consistent with the far-field distribution is imposed, Eq. (7) should be replaced by Eq. (9). In this case, Eqs. (A.1), (A.2a), (A.4) and (A.13b)–(A.13d) are still applicable, while Eq. (A.13a) becomes

$$|z| = b: \quad C_w^{(i)} = -C_p^{(i)}. \tag{A.21}$$

With this change, it can be shown that the results of the reflected fields and of the particle velocity are also obtained from Eq. (A.14)–(A.20) by replacing G and d_1 by $-G$ and $\bar{d}_1$, respectively, where

$$\bar{d}_1 = \int_0^\infty \frac{\rho^2}{e^{2\rho}+1}\,d\rho = 0.225386. \tag{A.22}$$

Comparing Eq. (A.20) for the slit case with Eq. (A.11a) for the case of a single parallel plane, one can find that the wall effects on the diffusiophoretic velocity of a particle in the two cases are qualitatively similar. However, the assumption that the result of the boundary effect for two walls can be obtained by simple addition of the single-wall effects generally gives a smaller correction to diffusiophoretic velocity, while for the corresponding sedimentation problem this approximation overestimates the wall correction.

Appendix B. Definitions of some functions in Section 2

The functions $\delta_n^{(i)}$ with $i = 1, 2, 3$, and 4 in Eqs. (13), (14), and (21) are defined by

$$\delta_n^{(1)}(r,\mu) = r^{-n-1}P_n^1(\mu) - (-n)^m\int_0^\infty \kappa^{1-m}\frac{J_1(\kappa\rho)}{\sinh\tau} \times[c^2 V_{n+m}(c)(\sinh\sigma)^{1-m}(\cosh\sigma)^m - b^2 V_{n+m}(-b)(\sinh\omega)^{1-m}(\cosh\omega)^m]\,d\kappa, \tag{B.1}$$

$$\delta_n^{(2)}(r,\mu) = -(n+1)r^{-n-2}P_n^1(\mu) - (-n)^m\int_0^\infty \frac{\kappa^{2-m}}{\sinh\tau} \times\{J_1'(\kappa\rho)(1-\mu^2)^{1/2}[c^2 V_{n+m}(c)(\sinh\sigma)^{1-m} \times(\cosh\sigma)^m - b^2 V_{n+m}(-b)(\sinh\omega)^{1-m} \times(\cosh\omega)^m] + J_1(\kappa\rho)\mu \times[c^2 V_{n+m}(c)(\cosh\sigma)^{1-m} \times(\sinh\sigma)^m - b^2 V_{n+m}(-b)(\cosh\omega)^{1-m} \times(\sinh\omega)^m]\}\,d\kappa, \tag{B.2}$$

$$\delta_n^{(3)}(r,\mu) = -r^{-n-1}\frac{\partial P_n^1(\mu)}{\partial\mu}(1-\mu^2)^{1/2} - (-n)^m r\int_0^\infty \frac{\kappa^{2-m}}{\sinh\tau}\{J_1'(\kappa\rho)\mu \times[c^2 V_{n+m}(c)(\sinh\sigma)^{1-m}(\cosh\sigma)^m - b^2 V_{n+m}(-b)(\sinh\omega)^{1-m}(\cosh\omega)^m] - J_1(\kappa\rho)(1-\mu^2)^{1/2}[c^2 V_{n+m}(c)(\cosh\sigma)^{1-m} \times(\sinh\sigma)^m - b^2 V_{n+m}(-b)(\cosh\omega)^{1-m} \times(\sinh\omega)^m]\}\,d\kappa, \tag{B.3}$$

$$\delta_n^{(4)}(r,\mu) = (n+1)(n+3)r^{-n-3}P_n^1(\mu) - (-n)^m \times \int_0^\infty \frac{\kappa^{3-m}}{\sinh\tau}\{[J_1''(\kappa\rho)(1-\mu^2) + J_1(\kappa\rho)\mu^2] \times[-c^2 V_{n+m}(\sinh\sigma)^{1-m}(\cosh\sigma)^m - b^2 V_{n+m}(-b)(\sinh\omega)^{1-m}(\cosh\omega)^m] + 2J_1'(\kappa\rho)(1-\mu^2)^{1/2}\mu[c^2 V_{n+m}(c)(\cosh\sigma)^{1-m} \times(\sinh\sigma)^m - b^2 V_{n+m}(-b)(\cosh\omega)^{1-m} \times(\sinh\omega)^m]\}\,\mathrm{d}\kappa. \quad \text{(B.4)}$$

Here,

$$V_n(z_i) = \frac{(2/\pi)^{1/2}}{z_i^{n+1}} \sum_{q=0}^{[n/2]} \frac{(\kappa|z_i|)^{n-q-1/2}}{(-2)^q q!(n-2q-1)!} \times K_{n-q-3/2}(\kappa|z_i|), \quad \text{(B.5)}$$

$$\sigma = \kappa(z+b), \quad \omega = \kappa(z-c), \quad \tau = \kappa(b+c), \quad \text{(B.6a–c)}$$

J_1 is the Bessel function of the first kind of order one and the prime on it denotes differentiation with respect to its argument, K_v is the modified Bessel function of the second kind of order v, and the square bracket $[v]$ denotes the largest integer which is less than or equal to v. In Eqs. (B.1)–(B.4), $m = 1$ if Eq. (7) is used for the boundary condition of the solute concentration field at the plane walls and $m = 0$ if Eq. (9) is used.

References

Anderson, J. L. (1989). Colloid transport by interfacial forces. *Annual Review of Fluid Mechanics*, *21*, 61–99.

Anderson, J. L., Lowell, M. E., & Prieve, D. C. (1982). Motion of a particle generated by chemical gradients. Part 1. Non-electrolytes. *Journal of Fluid Mechanics*, *117*, 107–121.

Anderson, J. L., & Prieve, D. C. (1991). Diffusiophoresis caused by gradients of strongly adsorbing solutes. *Langmuir*, *7*, 403–406.

Chen, S. B., & Keh, H. J. (1999). In J. Hsu (Ed.), *Interfacial forces and fields*. New York: Dekker.

Dukhin, S. S., & Derjaguin, B. V. (1974). Electrokinetic phenomena. In E. Matijevic (Ed.), *Surface and colloid science*, vol. 7. New York: Wiley.

Ebel, J. P., Anderson, J. L., & Prieve, D. C. (1988). Diffusiophoresis of latex particles in electrolyte gradients. *Langmuir*, *4*, 396–406.

Ganatos, P., Weinbaum, S., & Pfeffer, R. (1980). A strong interaction theory for the creeping motion of a sphere between plane parallel boundaries. Part 2. Parallel motion. *Journal of Fluid Mechanics*, *99*, 755–783.

Happel, J., & Brenner, H. (1983). *Low Reynolds number hydrodynamics*. Dordrecht, The Netherlands: Nijhoff.

Keh, H. J., & Chen, S. B. (1988). Electrophoresis of a colloidal sphere parallel to a dielectric plane. *Journal of Fluid Mechanics*, *194*, 377–390.

Keh, H. J., & Hsu, J. H. (2000). Boundary effects on diffusiophoresis of cylindrical particles in nonelectrolyte gradients. *Journal of Colloid and Interface Science*, *221*, 210–222.

Keh, H. J., & Jan, J. S. (1996). Boundary effects on diffusiophoresis and electrophoresis: Motion of a colloidal sphere normal to a plane wall *Journal of Colloid and Interface Science*, *183*, 458–475.

Keh, H. J., & Luo, S. C. (1995). Particle interactions in diffusiophoresis in nonelectrolyte gradients. *Physics of Fluids*, *7*, 2122–2131.

O'Brien, V. (1968). Form factors for deformed spheroids in Stokes flow. *AIChE Journal*, *14*, 870–875.

O'Brien, R. W. (1983). The solution of the electrokinetic equations for colloidal particles with thin double layers. *Journal of Colloid and Interface Science*, *92*, 204–216.

O'Neill, M. E. (1964). A slow motion of viscous liquid caused by a slowly moving solid sphere. *Mathematika*, *11*, 67–74.

Staffeld, P. O., & Quinn, J. A. (1989). Diffusion-induced banding of colloid particles via diffusiophoresis. 2. Non-electrolytes. *Journal of Colloid and Interface Science*, *130*, 88–100.